Biotin Synthase Mechanism: Mutagenesis of the YNHNLD Conserved Motif[†,‡]

Manuela Lotierzo,[▽,§] Evelyne Raux,[||] Bernadette Tse Sum Bui,[▽] Nicole Goasdoue,[▽] Francine Libot,[⊥] Dominique Florentin,[▽] Martin J. Warren,[||] and Andrée Marquet*[,▽]

Université Pierre et Marie Curie-Paris 6, CNRS UMR 7613, (Synthèse, Structure et Fonction de Molécules Bioactives), FR2769, Case Courrier 182, 4 place Jussieu, 75005 Paris, France, University of Kent, Department of Bioscience, Canterbury, Kent CT2 7NJ, U.K., and Université René Descartes, CNRS UMR 8638, Laboratoire de Pharmacognosie, 4, Avenue de l'Observatoire, F-75006 Paris, France

Received April 4, 2006; Revised Manuscript Received August 1, 2006

ABSTRACT: Biotin synthase, a member of the "radical SAM" family, catalyzes the final step of the biotin biosynthetic pathway, namely, the insertion of a sulfur atom into dethiobiotin (DTB). The active form of the enzyme contains two iron−sulfur clusters, a $[4Fe\text{-}4S]^{2+}$ cluster liganded by Cys-53, Cys-57, and Cys-60 and the *S*-adenosylmethionine (AdoMet or SAM) cosubstrate and a $[2Fe\text{-}2S]^{2+}$ cluster liganded by Cys-97, Cys-128, Cys-188, and Arg-260. Single-point mutation of each of these six conserved cysteines produced inactive variants. In this work, mutants of other highly conserved residues from the Y^{150}NHNLD motif are described. They have properties similar to those of the wild-type enzyme with respect to their cluster content and characteristics. For all of them, the as-isolated form, which contains an air-stable $[2Fe\text{-}2S]^{2+}$ center, can additionally accommodate an air-sensitive $[4Fe\text{-}4S]^{2+}$ center which is generated by incubation under anaerobic conditions with Fe^{2+} and S^{2-}. Their spectroscopic properties are similar to those of the wild type. However, they are inactive, except the mutant H152A that exhibits a weak activity. We show that the mutants, inactive in producing biotin, are also unable to cleave AdoMet and to produce the deoxyadenosyl radical ($AdoCH_2^{\bullet}$). In the case of H152A, a value of 5.5 ± 0.4 is found for the 5′-deoxyadenosine ($AdoCH_3$):biotin ratio, much higher than the value of 2.8 ± 0.3 usually observed with the wild type. This reveals a greater contribution of the abortive process in which the $AdoCH_2^{\bullet}$ radical is quenched by hydrogen atoms from the protein or from some components of the system. Thus, in this case, the coupling between the production of $AdoCH_2^{\bullet}$ and its reaction with the hydrogen at C-6 and C-9 of DTB is less efficient than that in the wild type, probably because of geometry's perturbation within the active site.

Biotin synthase (BioB),[1] which catalyzes the last step of biotin biosynthesis (Scheme 1) (*1*−*3*), is a member of the "radical SAM" superfamily (*4*).

This group of enzymes uses *S*-adenosylmethionine (SAM or AdoMet) as a cofactor. Their main signature is the C-X_3-C-X_2-C motif (Cys-53, Cys-57, and Cys-60 in *Escherichia coli* biotin synthase) (*4*). It is now established that these conserved cysteines are ligands to a $[4Fe\text{-}4S]^{2+}$ cluster

Scheme 1: Reaction Catalyzed by Biotin Synthase

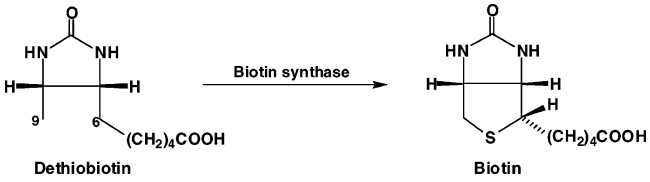

present in all the already characterized enzymes which is likely to be the case for the whole family. This appears clearly in the recently determined crystal structures of four members of the family (*5*−*8*), which also show that the ligand of the fourth iron is AdoMet, coordinated by both its carboxylate and amino groups. The role of this cluster is to mediate, via flavodoxin (*9*) and flavodoxin reductase (*10*), the one-electron transfer from NADPH to AdoMet. This initiates its cleavage into methionine and a deoxyadenosyl radical ($AdoCH_2^{\bullet}$) (*11*−*13*). The other conserved cysteines of biotin synthase, Cys-97, Cys-128, and Cys-188, are ligands to a $[2Fe\text{-}2S]^{2+}$ center, which is specific to this enzyme.

A consistent mechanistic picture is now emerging for biotin synthase (*14*, *15*) (Scheme 2). The as-isolated enzyme is a homodimer which contains the air-stable $[2Fe\text{-}2S]^{2+}$ center (one cluster per monomer) (*16*−*18*). The air-sensitive $[4Fe\text{-}4S]^{2+}$ cluster is not present after aerobic purification,

[†] This research has been supported in part by the European Community's Human Potential Programme under Contract HPRN-CT-2002-00244 (Viteomics). M.L. acknowledges the postdoctoral fellowship provided by this contract.

* To whom correspondence should be addressed. Telephone: +33 1 44 27 31 13. Fax: +33 1 44 27 38 43. E-mail: marquet@ccr.jussieu.fr.

[‡] We dedicate this paper to the memory of Anne Vidal-Cros.

[▽] Université Pierre et Marie Curie-Paris 6.

[§] Present address: Département d'ingénierie et d'étude des protéines (DIEP), CEA/Saclay, 91191 Gif-sur-Yvette Cedex, France.

[||] University of Kent.

[⊥] Université René Descartes, UMR CNRS 8638.

[1] Abbreviations: BioB, biotin synthase; AdoMet or SAM, *S*-adenosylmethionine; NADPH, nicotinamide adenine dinucleotide phosphate, reduced form; $AdoCH_2^{\bullet}$, 5′-deoxyadenosyl radical; DTT, dithiothreitol; DTB, dethiobiotin; LipA, lipoyl synthase; CD, circular dichroism; WT, wild-type; $AdoCH_3$, 5′-deoxyadenosine; dNTP, deoxyribonucleotide triphosphate; SDS−PAGE, sodium dodecyl sulfate−polyacrylamide gel electrophoresis; Tris-HCl, tris(hydroxymethyl)-aminomethane hydrochloride; CID, collision-induced dissociation.

10.1021/bi060662m CCC: $33.50
Published on Web 09/14/2006

Scheme 2: Proposed Mechanism for the Formation of Biotin from DTB

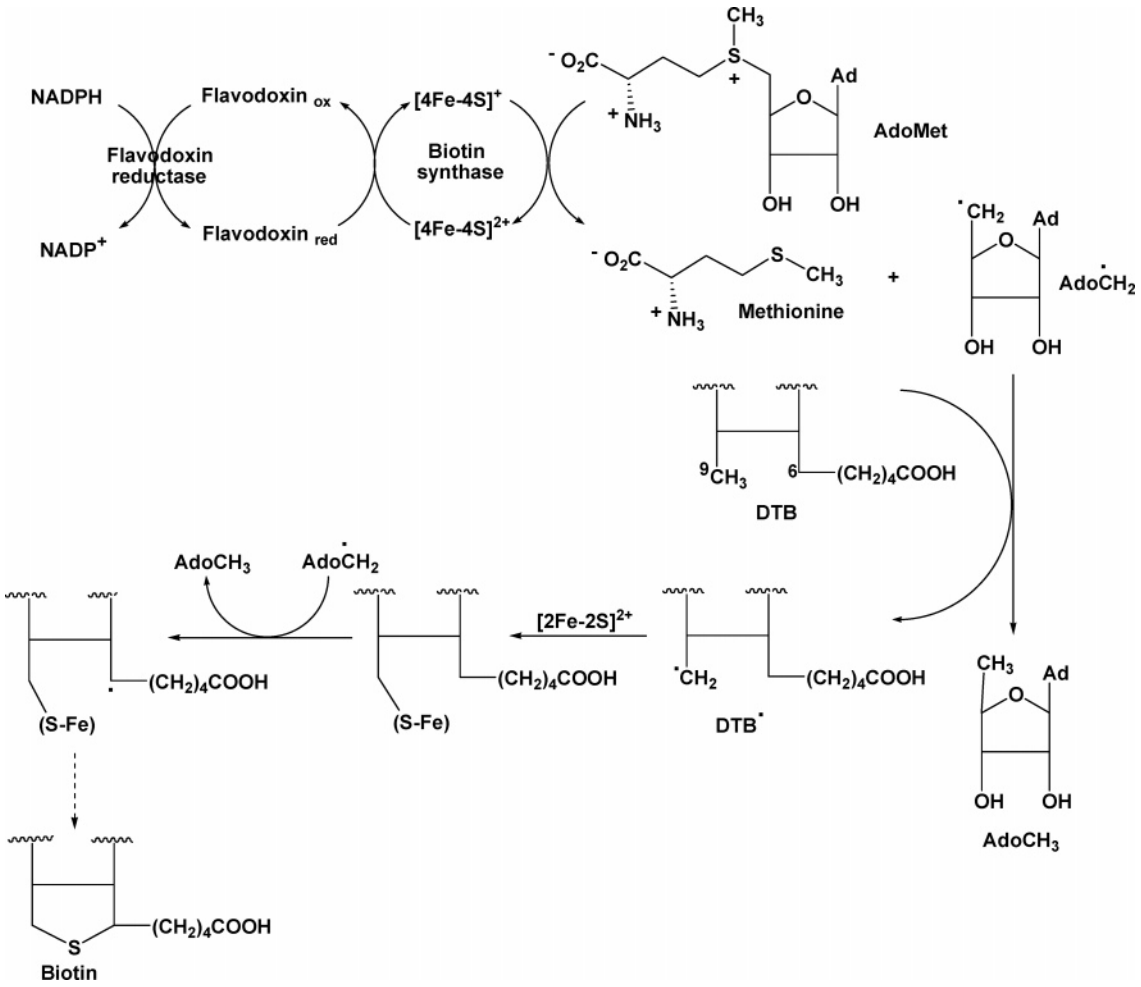

but it can be reconstituted in the as-isolated form of the enzyme by incubation, under strictly anaerobic conditions, with an excess of Fe^{2+} or Fe^{3+} and S^{2-}, in the presence of dithiothreitol (DTT) (*19*, *20*). The presence of both $[2Fe\text{-}2S]^{2+}$ and $[4Fe\text{-}4S]^{2+}$ centers is essential for activity (*14*, *15*, *21*). $AdoCH_2^{\bullet}$ formed by the reduction of AdoMet abstracts a hydrogen at C-9 of dethiobiotin (DTB), and the resulting $DTB^{\bullet}$ quenches a sulfur atom (*22*). Evidence of the participation of the $[2Fe\text{-}2S]^{2+}$ center as the sulfur donor, to give an intermediate whose chemical nature is not yet defined, exists (*15*, *17*, *20*). A second $AdoCH_2^{\bullet}$ is generated from another AdoMet, producing a radical at C-6 of this intermediate, resulting in the ring closure (*22*).

In previous studies, the conserved cysteines, Cys-53, Cys-57, Cys-60, Cys-97, Cys-128, and Cys-188, have been replaced either with alanine (*23*, *24*) or with serine (*25*). Not surprisingly, since these residues act as ligands for the essential [Fe-S] clusters, all these mutants were inactive. The discussion of their spectroscopic properties is not straightforward, according to what is now known about the complexity of the iron−sulfur cluster system. Another highly conserved region in BioB is the "Tyr-150/Asn-151/His-152/Asn-153/Leu-154/Asp-155" sequence (YNHNLD) which is also found in lipoyl synthase (LipA) (*1*) as "FNHNLE" (residues 191−196 in *E. coli*). The crystal structure of biotin synthase (*6*) shows that Asn-151, Asn-153, and Asp-155 have their side chains oriented toward the active site, in a position to form hydrogen bonds with either the substrate DTB or

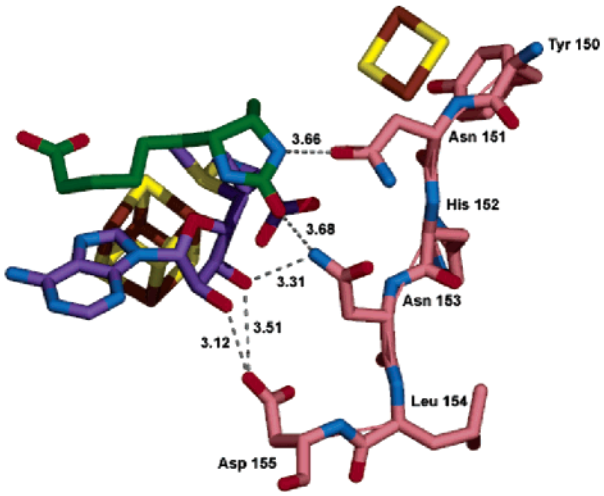

FIGURE 1: View of DTB (carbons colored green) and SAM (carbons colored violet) interacting with the residues of the Tyr-150/Asn-151/His-152/Asn-153/Leu-154/Asp-155 (carbons colored salmon) sequence in the active site: O, red; N, blue; S, yellow; and Fe, brown. This figure was generated and rendered with PyMOL (*26*).

the cosubstrate AdoMet. On the other hand, the side chains of Tyr-150, His-152, and Leu-154 are oriented in the opposite direction (Figure 1). In this study, we have mutated four different amino acids of this motif (Asn-151, His-152, Asn-153, and Asp-155) to Ala and characterized these variant BioB enzymes. Among them, only His-152 does not seem

to be in the position to form any hydrogen bond as it has the side chain oriented away from the active site.

The mutant enzymes were characterized by iron analysis, UV−visible, and circular dichroism (CD), and their activity was determined. Although chromatographic profiles, CD spectra, and [Fe-S] cluster reconstitution showed the enzymes were highly similar to wild-type BioB, the mutants N151A, N153A, and D155A were inactive in producing biotin, within the microbiological test detection limit. The H152A mutant exhibited an activity, but only approximately 10% of that of the wild-type enzyme. For each mutant, including the inactive ones, we examined if 5′-deoxyadenosine ($AdoCH_3$) was produced, since the mutation could affect any of the partial reactions of the pathway, and AdoMet could be cleaved even though no biotin was formed. $AdoCH_3$ was detected for only the active mutant (H152A) and not for the three others. An $AdoCH_3$:biotin ratio of 5.5 ± 0.4 was calculated for H152A, showing a rate of consumption of the deoxyadenosyl radical higher than that found for the wild-type protein (2.8 ± 0.3 mol of $AdoCH_3$/mol of biotin). This probably reveals a perturbation of the geometry within the active site.

MATERIALS AND METHODS

Materials. Chemicals were purchased either from Sigma-Aldrich Chemical Co., VWR International, or Acros Organics unless otherwise stated. $AdoCH_3$ was synthesized in our laboratory (*11*).

Strain and Plasmid. E. coli strain BL21(DE3)pLysS pJJ15-4A overexpressing biotin synthase bearing a His_6 tag at its N-terminus (*27*, *28*) was a generous gift from J. Jarrett (University of Pennsylvania, Philadelphia, PA).

Construction of Mutants. Site-directed mutagenesis was performed using the GeneEditor in vitro site-directed mutagenesis system (Promega) for the N151A and N153A mutations and QuickChange site-directed mutagenesis kit (Stratagene) for the H152A and D155A mutations. Oligonucleotides for mutagenesis were purchased from Invitrogen. All mutations were verified by DNA sequencing (MilleGen). The asparagines from the YNHNLD sequence were mutated individually to alanine. The GeneEditor protocol from Promega was followed: the selection oligonucleotide (2.9 ng), encoding mutations that alter the ampicillin resistance gene to create a new additional resistance to the GeneEditor antibiotic selection mix, was annealed to wild-type plasmid pJJ15-4A (approximately 2 μg) at the same time as a mutagenic oligonucleotide (14 ng), previously phosphorylated at the 5′ position. Subsequent elongation from the two oligonucleotides and ligation followed to create a circular new strand, and then *E. coli* BMH 71-18 *mutS* competent cells were transformed with this plasmid. A second transformation into *E. coli* JM109 ensures segregation of mutant and wild-type plasmids; a final transformation in *E. coli* BL21(DE3)pLysS (Promega) was carried out for protein expression: target primer for N151A, CGGGCTGGATTACTACGCGCACAACCTGGACACC; target primer for N153A, GATTACTACAACCACGCGCTGGACACCTCGCCG (mutations underlined).

His-152 and Asp-155 from the YNHNLD sequence were also mutated to alanine; 125 ng of two complementary oligonucleotides, each containing the desired mutation of a single nucleotide, was thermocycled along with 50 ng of wild-type plasmid pJJ15-4A, 1 μL of dNTP mix, 5 μL of reaction buffer, and 2.5 units of *Pfu*Turbo DNA polymerase in a total volume of 50 μL. The mixture was heated to 95 °C for 30 s, followed by 16 cycles of 95 °C for 30 s, 55 °C for 1 min, and 68 °C for 6 min, as suggested by the QuickChange protocol. The resulting PCR mixture was digested with *Dpn*I to nick the original template plasmid. Primers were constructed as follows: BioB H152A sense/antisense primer pair, 5′-CTGGATTACTACAACGCCAACCTGGACACCTC-3′/5′-GAGGTGTCCAGGTTGGCGTTGTAGTAATCCAG-3′; BioB D155A sense/antisense primer pair, 5′-CAACCACAACCTGGCCACCTCGCCGGAG-3′/5′-CTCCG-GCGAGGTGGCCAGGTTGTGGTTG-3′. Corresponding plasmids were selected in *E. coli* XL1-Blue supercompetent cells followed by transformation into *E. coli* BL21(DE3)pLysS for protein expression.

Expression, Purification, and Characterization of Wild-Type BioB and Mutants. Proteins overproduction and purification were carried out as previously described (*27*, *28*). All buffers were saturated with argon before being used. Cells were resuspended in 50 mM Tris-HCl (pH 8) (buffer A) and sonicated under a refrigeration system with propan-2-ol at 4 °C. After centrifugation to remove cell debris, the supernatant was diluted with 3 volumes of buffer A and centrifuged again. The diluted cell-free extract was loaded onto a Ni^{2+}-chelating Sepharose (Pharmacia-Amersham) column (2.5 cm × 5 cm), previously equilibrated with buffer A containing 0.5 M NaCl and 100 mM imidazole. Under the conditions that were used, most of the contaminating proteins did not bind and were eliminated in the nonretained fraction. Bound proteins were eluted with the same buffer containing 200 mM imidazole. After concentration on Centriprep 30 concentrators (Millipore), the enzyme was desalted on a Sephadex G-25 column equilibrated with buffer A and further concentrated to 242 μM, frozen in liquid nitrogen, and stored at −80 °C until further use. UV−visible spectra were measured over the scan range of 250−700 nm using a Uvikon 930 spectrophotometer.

Enzymatic Assays and $AdoCH_3$ Quantification. An activity test of the five enzymes was performed as previously described (*28*). Both microbiological tests with *Lactobacillus plantarum* (*29*) and HPLC analysis were used for quantification of the produced biotin. The two detection methods gave comparable results, the difference not exceeding 5% (*30*).

For the quantification of $AdoCH_3$, 25 μL of 12% trichloroacetic acid was added to 250 μL aliquots of the enzymatic assay mixture to quench the reaction. Precipitated proteins were pelleted by centrifugation, and 200 μL of the supernatant was analyzed using a HPLC reversed phase C18 Nucleosil 100-5 Å, 250 mm × 4 mm column (Macherey-Nagel). The solvent system consisted of 100% H_2O (eluent A) and H_2O with acetonitrile (60:40, v/v) (eluent B). Separations were made at a flow rate of 1.2 mL/min using a 30 min linear gradient beginning with 100% eluent A and ending with 100% eluent B. The optical density was monitored at 259 nm. The retention time for $AdoCH_3$ was approximately 14 min. The area of the HPLC peak corresponding to $AdoCH_3$ was measured and the concentration calculated from a calibration curve in a range of 2.5−50 μM. Aliquots of $AdoCH_3$ were collected, evaporated to dryness using a Jouan RC 10.10 vacuum centrifuge, and dissolved in acetonitrile for mass spectroscopy analysis. Positive ESI

mass spectra were acquired using a Q-TOF mass spectrometer (Micromass) with an ESI-Z spray source, operating in Masslynx 4.0. Solutions of samples (100 μmol/L) in CH_3CN were introduced by infusion into the ionization chamber under atmospheric pressure via a syringe pump at a rate of 10 μL/min. Collision-induced dissociation (CID) spectra were recorded using argon as the collision gas.

Preparation and Characterization of Reconstituted Enzymes. Aliquots (500 μL) of enzymes (240 μM), 250 mM DTT, 40 mM $Fe(NH_4)_2(SO_4)_2$, and 40 mM Na_2S were degassed separately for 30 min at room temperature under a stream of moist argon and then transferred to a glovebox (Jacomex BS531 NMT, $[O_2] < 2$ ppm) at ca. 15 °C overnight. After this time, DTT to a final concentration of 5 mM and 5-fold excesses of $Fe(NH_4)_2(SO_4)_2$ and Na_2S with respect to the enzyme were added to the solution. The mixture was incubated for 3 h at room temperature and then desalted in the glovebox on a Sephadex G-25 column with anaerobic 50 mM Tris-HCl buffer (pH 7.5). A volume of 1 mL of the enzyme solution at a concentration of 24.2 μM was transferred to quartz cuvettes, and the cuvettes were capped with an airtight rubber septum for recording UV−visible spectra. The spectra of the as-isolated enzymes, obtained from the same purification batch, were also recorded.

Analytical Methods. Protein concentrations were determined by the method of Bradford (*31*), using bovine serum albumin as a standard. BioB concentrations were expressed per 41.3 kDa monomer (*27*). The amount of Fe was determined by the method of Fish (*32*).

RESULTS

Mutagenesis of Asn-151, His-152, Asn-153, and Asp-155 in the Conserved Motif. To investigate the role of the YNHNLD motif that is highly conserved in BioB proteins, four of these residues were individually mutated: N151A, H152A, N153A, and D155A. Cells containing the wild-type and mutant constructs gave a comparable level of protein expression. The mutants exhibited chromatographic properties similar to those of the wild type during purification, having similar elution profiles from the Ni^{2+}-chelating Sepharose columns. All five enzymes were isolated in a highly pure form, as judged by SDS−PAGE, and had a similar reddish brown coloration due to the presence of the $[2Fe\text{-}2S]^{2+}$ cluster. The nature and the amount of cluster were further investigated by iron quantification, UV−visible spectrometry (Figure 2), and CD spectrometry (Supporting Information). The iron content of the as-isolated forms of the four mutants (Table 2) was similar, ranging from 1.0 to 1.6 mol of iron/mol of BioB monomer. The UV−visible spectra of the as-isolated enzymes show characteristic peaks for the $[2Fe\text{-}2S]^{2+}$ clusters at 330, 420, and 453 nm exhibit similar features, and the cluster:protein ratio for the mutants is comparable to that of the wild type (WT) (Table 1).

A higher value of the three ratios was found for N151A, with respect to the WT. A lower value was observed, on the other hand, in the case of D155A. This probably reflects larger and smaller amounts of cluster, respectively. The CD spectra of the five proteins were also recorded, in the 200−250 nm range for analysis of the fold of the proteins and in the 300−600 nm range for an investigation of the iron−sulfur cluster (*33*). No significant changes were observed either in the near-UV or in the visible region, suggesting that the mutant variants had adopted a fold similar to that of the wild-type protein and a similar arrangement around the cluster (Supporting Information).

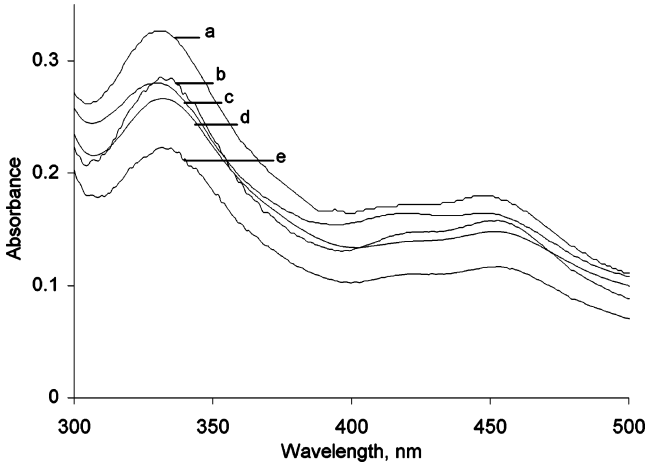

FIGURE 2: UV−visible spectra of as-isolated BioB enzymes. (d) Wild-type, (a) N151A, (b) H152A, (c) N153A, and (e) D155A mutants. All enzymes (24.2 μM) had the same ϵ value at 278 nm.

Table 1: Absorption Properties of the As-Isolated Form of Wild-Type *E. coli* BioB and Mutants

	A_{330}/A_{278}	A_{420}/A_{278}	A_{453}/A_{278}
WT	0.38 ± 0.05	0.20 ± 0.03	0.21 ± 0.02
N151A	0.45 ± 0.05	0.24 ± 0.05	0.25 ± 0.01
H152A	0.39 ± 0.03	0.20 ± 0.02	0.22 ± 0.04
N153A	0.39 ± 0.08	0.24 ± 0.05	0.24 ± 0.03
D155A	0.32 ± 0.04	0.16 ± 0.02	0.17 ± 0.02

Table 2: Comparison between Wild-Type BioB and Mutants[a]

	iron content/monomer[b]			
	as-isolated	after reconstitution	biotin, μM	$AdoCH_3$/biotin
WT	1.5 ± 0.1	7.0 ± 0.1	9.8 ± 0.4	2.8 ± 0.3
N151A	1.4 ± 0.2	7.1 ± 0.3	<0.25	−
H152A	1.6 ± 0.2	8.2 ± 0.5	1.3 ± 0.4	5.5 ± 0.4
N153A	1.0 ± 0.1	6.9 ± 0.1	<0.25	−
D155A	1.4 ± 0.2	5.5 ± 0.5	<0.25	−

[a] Data are means from at least three independent experiments with each one performed in duplicate or triplicate. [b] The presence in all samples of small amounts of nonspecific iron cannot be excluded.

Activity of the Mutants. The mutant enzymes were tested for their activity (Table 2), using the established assay conditions with the same protein concentration (10 μM). No biotin was detected in the assays for three of the four mutants: N151A, N153A, and D155A. Only the H152A protein exhibited a small activity with formation of 1.3 ± 0.4 μM biotin corresponding to an enzyme turnover approximately $^1/_{10}$ of that observed with the wild type. As outlined earlier, the transformation of dethiobiotin into biotin is a complex process, and the absence of biotin in the mutant assays could be due to a blockage at one of a number of steps, for instance, in the reduction of AdoMet, in the hydrogen abstraction from DTB by $AdoCH_2^{\bullet}$, or in the sulfur insertion (Scheme 2). Thus, we investigated if $AdoCH_3$ was produced during reaction with the "inactive" mutants. When the supernatant of the assays with N151A, N153A, and

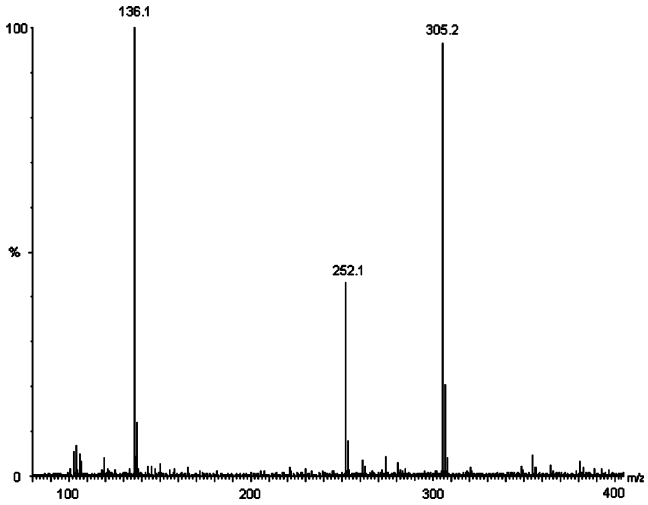

FIGURE 3: Positive ESI mass spectrum of collected $AdoCH_3$ in acetonitrile (cone voltage of 60 V).

D155A was analyzed by HPLC, no $AdoCH_3$ was detected, meaning that the first step, the cleavage of AdoMet, had not taken place. If $AdoCH_2^{\bullet}$ had been produced but had not reacted with DTB, chemical logic dictates that it would have reacted with some residues of the protein, resulting in the formation of $AdoCH_3$ in any case. On the other hand, in the reaction with H152A, a peak with a retention time identical to that of authentic $AdoCH_3$ was present. It was collected and analyzed by mass spectrometry to ensure that it contained pure $AdoCH_3$. The positive ESI mass spectrum reported in Figure 3 shows that this sample does indeed contain $AdoCH_3$, characterized by its protonated form $[AdoCH_3H^+]$ at *m*/*z* 252 and its diagnostic fragment ion $[C_5H_5N_5]H^+$ at *m*/*z* 136 (*22*), and also some polyethylene glycol {polyethylene glycol is ionized by a sodium ion $[H(OCH_2CH_2)_6OH]Na^+$ at *m*/*z* 305, and its structure was confirmed by CID experiments of the MH^+ ion at *m*/*z* 283 formed after addition of a 0.5% formic acid solution (data not shown)}. Nevertheless, this impurity does not contribute to the absorption at 259 nm. Therefore, the quantity of $AdoCH_3$ was determined from the HPLC chromatogram using a calibration curve with authentic $AdoCH_3$.

Interestingly, the $AdoCH_3$:biotin ratio was found to be 5.5 $\pm$ 0.4 for the H152A variant, whereas it is only 2.8 $\pm$ 0.3 with the wild type (Table 2). Successive reactions of $AdoCH_2^{\bullet}$ with a hydrogen at C-9 and then at C-6 of DTB should produce 2 $AdoCH_3$ molecules per biotin. The observed value of 2.8 means that some abortive process is taking place, i.e., abstraction of hydrogen from the protein. The much higher value of 5.5 $\pm$ 0.4 found with the mutant shows a greater participation of the abortive process.

Preparation of Reconstituted Enzymes and Spectroscopic Characterization. In the mechanism of BioB, the $[4Fe\text{-}4S]^{2+}$ cluster is responsible for the electron transfer which leads to AdoMet cleavage, producing the deoxyadenosyl radical. We investigated if the failure of the inactive mutants to perform this reductive cleavage is due to their inability to reconstitute this cluster during the enzymatic assay. Each of the as-isolated BioB enzymes was incubated with $Fe(NH_4)_2(SO_4)_2$, Na_2S, and DTT in anaerobic Tris-HCl buffer (pH 7.5). After incubation for 3 h inside the nitrogen glovebox ($[O_2] < 2$ ppm), the reagent excess was removed by gel filtration chromatography (still within the glovebox). Analysis of the iron content in the resulting proteins confirmed that an additional cluster had been reconstituted. The D155A mutant contained less iron (5.5 $\pm$ 0.5 Fe atoms/monomer) than the wild-type preparation (7.0 $\pm$ 0.1 Fe atoms/monomer) or the other mutants (Table 2). All proteins had a broad absorption band from 380 to 420 nm, characteristic of $[4Fe\text{-}4S]^{2+}$ centers. UV−visible spectra for the reconstituted enzymes are shown in Figure 4 and are markedly different from those of the as-isolated enzymes (Figure 2).

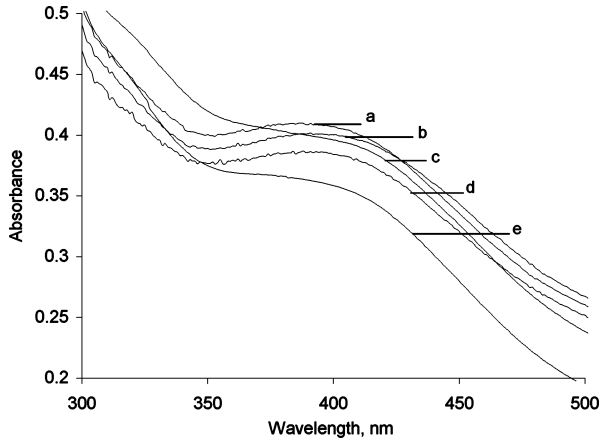

FIGURE 4: UV−visible spectra of the reconstituted BioB enzymes. (d) Wild-type, (a) D155A, (b) N151A, (c) N153A, and (e) H152A mutants. All enzymes (24.2 μM) had the same ϵ values at 278 nm.

The A_{410}/A_{278} ratio which is considered to correlate with the amount of $[4Fe\text{-}4S]^{2+}$ cluster per protein monomer is slightly different in each variant but clearly higher than those obtained with the as-isolated enzymes. Therefore, all the mutant variants are able to accommodate both the $[2Fe\text{-}2S]^{2+}$ and $[4Fe\text{-}4S]^{2+}$ centers.

DISCUSSION

The mechanism of action of biotin synthase has been the subject of highly controversial discussions. A consensus mechanistic picture is now emerging, but several aspects are still elusive. Site-directed mutagenesis, an obvious tool for mechanistic studies, has not been extensively exploited for biotin synthase. The two published studies involving mutation on BioB concern the conserved cysteines, which have been replaced with alanine or serine. Point mutations of cysteines 53, 57, 60, 97, 128, and 188 gave inactive variants. As this work was carried out before it was initially recognized by Jarrett's group (*14*, *19*) and further confirmed by the X-ray structure (*6*) that biotin synthase contains two [Fe-S] clusters, each with a specific function, the discussion of the spectroscopic properties of the mutants has to be reconsidered.

We know now that cysteines 53, 57, and 60 are ligands to the $[4Fe\text{-}4S]^{2+}$ center, whereas cysteines 97, 128, and 188 are ligands to the $[2Fe\text{-}2S]^{2+}$ center. Baxter's group (*25*) reported that the as-isolated C53S, C57S, and C60S mutant proteins do not contain any [Fe-S] center, while the wild type contains, as expected, the $[2Fe\text{-}2S]^{2+}$ cluster. Furthermore, no cluster could be reconstituted in the apoprotein. We have previously shown that incubation of the apoprotein with Fe^{3+}, S^{2-}, and DTT in the presence of traces of oxygen, i.e., under a stream of moist argon instead of inside a glovebox, gives a $[2Fe\text{-}2S]^{2+}$ cluster-containing enzyme, the properties and activity of which are quite similar to those of

the as-isolated form (*17*, *18*, *34*). The authors did not mention if they operated in a glovebox, and we can assume that, under the conditions that were used, they should have reconstituted the $[2Fe\text{-}2S]^{2+}$ center, the ligands of which were not mutated. We should thus conclude from these data that mutation of any Cys of the $[4Fe\text{-}4S]^{2+}$ cluster introduces a strong perturbation into the active site, preventing the formation of the $[2Fe\text{-}2S]^{2+}$ cluster. This is not consistent with the results observed in the groups of Roach and Fontecave (*23*, *24*) with the C53A, C57A, and C60A mutants, which appear to be more coherent. They isolated variant proteins containing apparently some $[2Fe\text{-}2S]^{2+}$ cluster. Reconstitution of the apoprotein forms under strictly anaerobic conditions gives a $[4Fe\text{-}4S]^{2+}$ cluster different from that of the wild type since it cannot be reduced. On the other hand, the mutation of the three other cysteines (the ligands to the $[2Fe\text{-}2S]^{2+}$ cluster) leads to a protein that can accommodate a reducible $[4Fe\text{-}4S]^{2+}$ cluster (*24*). It is difficult to know whether the difference between the two sets of results is due to the nature of the amino acid introduced into the mutants (Ala or Ser) or to the working conditions.

No mutagenesis study has yet been reported for the other conserved motif, YNHNLD, and there are no experimental data concerning its role. The X-ray structure (*6*) reveals that it belongs, as expected, to the active site. The side chains of the two asparagines, Asn-151 and Asn-153, and that of Asp-155 are oriented toward the active site (Figure 1). The NH_2 group of Asn-153 and the 3′-OH group of the AdoMet ribose ring as well as the OH group of Asp-155 and the 2′- and 3′-OH groups of this ring are in the position to form hydrogen bonds. The ureido moiety of DTB can also interact through its carbonyl group with the NH_2 group of Asn-153 and through one of its NH groups with the carbonyl of Asn-151.

We have now mutated these three amino acids into alanine and characterized the corresponding mutants. Also, according to the crystal structure, the three other residues of the motif, Tyr-150, His-152, and Leu-154, point out of the active site and do not form hydrogen bonds with DTB and SAM. Thus, their mutation should have less influence on the structure and activity of the corresponding variants. We selected one of these functionalized amino acids, namely, His-152, which was also mutated into alanine.

The first three mutants, N151A, N153A, and D155A, were completely inactive in the production of biotin; i.e., the amount of biotin produced was smaller than the detection limit (0.25 μM) which corresponds to a biotin:enzyme monomer ratio of 0.025. The fourth one, H152A, was active, but it had only $\sim 1/10$ of the activity of the wild-type enzyme.

However, the absence of biotin does not mean that the first steps of the reaction, for instance, the cleavage of SAM, do not take place. HPLC analysis of the assay supernatants revealed that no $AdoCH_3$ was present in the case of the three inactive mutants. We can conclude that no $AdoCH_2^{\bullet}$ has been produced, since it would necessarily end up as $AdoCH_3$, either by reaction with the substrate or through the abortive process. Such an abortive process takes place even with the wild type as shown by the $AdoCH_3$:biotin ratio, which was consistently 2.8 ± 0.3, whereas only 2 equiv of AdoMet should be consumed to react with the substrate. The excess is probably due to the quenching of the radical by a protein hydrogen (*11*, *22*) or by some components of the system. $AdoCH_3$ was found, as expected, in the supernatant of the assay with H152A. Interestingly, the $AdoCH_3$:biotin ratio was much higher than that found with the wild type, 5.5 ± 0.4 as opposed to 2.8 ± 0.3. This higher value reveals a larger contribution of the abortive process, which is competitive with the C−H bond cleavage of the substrate. We have observed that the same is true when dethiobiotin deuterated on the reactive positions is used as a substrate. This can be explained by an isotope effect for the cleavage of the C−D bond (D. Florentin et al., unpublished experiments). The lifetime of $AdoCH_2^{\bullet}$ is certainly very short, and reaction with the substrate has to be tightly coupled with its formation. One can anticipate that any factor that perturbs the optimal arrangement such as the difficulty of cleavage of the C−D bond with the labeled substrate, or a slight distortion of the geometry of the active site complex in the case of the H152A mutant, will increase the rate of the abortive processes with respect to the pathway leading to biotin.

The reasons for the inactivity of N151A, N153A, and D155A are still elusive. We investigated if it was related to a change in the nature and the amount of the [Fe-S] clusters they contained. The UV−visible spectra of the as-isolated mutant proteins are quite similar to that of the wild type and are characteristic of a $[2Fe\text{-}2S]^{2+}$ cluster. The absorbance values, as well as the iron content, indicate that the ratio of cluster to protein is very similar with the exception of that of the D155A variant, which is slightly reduced. Moreover the CD spectra reveal that the mutant variants have adopted an overall fold similar to that of the wild-type enzyme and that the cluster environment has not been significantly perturbed. These mutants have also preserved their ability to accommodate the $[4Fe\text{-}4S]^{2+}$ center after incubation in the glovebox ($[O_2] < 2$ ppm) with an excess of Fe^{2+} and S^{2-}, as shown by the UV−visible spectra and the determination of iron content. Thus, the mixed cluster state, which represents the active form, has been reconstructed. The absence of SAM cleavage by the first three mutants may reflect the absence of SAM binding. We have conducted EPR experiments with the five proteins, anaerobically isolated and reduced with dithionite, and we have observed that the nature and stability of the EPR signals corresponding to the [Fe-S] clusters of these enzymes were modified by the addition of SAM (and to a lesser extent by the addition of DTB), which implies its binding to the protein (M. Lotierzo, S.E.J. Rigby, et al., unpublished results). We thus favor the hypothesis that it is the reductive cleavage of SAM which is blocked in the inactive mutants. Only subtle changes in the geometry of the active site, due to the removal of some hydrogen bonds, could perhaps change the redox properties of the clusters.

The fourth mutant, H152A, with its imidazole ring oriented outside the active site was expected to be active. Its activity is low, however, only 10% of that of the wild type. It behaves like the other ones as far as the clusters are concerned. It is possible that the replacement of the protonatable imidazole with a methyl group suppresses a positive charge having a significant structural influence around the active site. This confirms that a full activity requires a perfectly positioned arrangement of all the components of the reactive complex. Nevertheless, these results do not explain why the concerned residues are essential. It should be pointed out that the YNHNLD sequence is also found in lipoyl synthase, the

second characterized enzyme involved in C−S bond formation, as FNHNLE.

It has been proposed that this motif could be involved in positioning $AdoCH_2^{\bullet}$ in the correct orientation for the abstraction of the C-6 and C-9 hydrogen atoms from DTB (*35*). However, as discussed by the authors, the substrate of lipoyl synthase has no functionality at this location. Furthermore, the fact that our mutants do not produce any $AdoCH_2^{\bullet}$ strongly suggests that its positioning within the active site is not the only role played by these amino acids in the wild type. It could be interesting to replace Asn-151, Asn-153, and Asp-155 not with Ala but with other residues which occupy an equivalent position with respect to SAM in the other SAM-dependent enzymes and see whether they recover the ability to cleave SAM.

ACKNOWLEDGMENT

We are grateful to Dr. Anne Vidal-Cros and Dr. Hubert Becker for their advice in molecular biology, to Dr. Denis Lesage for his help with mass spectrometry, and to Dr. Serge Fermandjian for providing CD spectrometry facilities.

SUPPORTING INFORMATION AVAILABLE

CD spectra of wild-type and mutant BioB in the 200−250 and 300−600 nm ranges. This material is available free of charge via the Internet at http://pubs.acs.org.

REFERENCES

1. Marquet, A., Tse Sum Bui, B., and Florentin, D. (2001) Biosynthesis of biotin and lipoic acid, in *Vitamins and Hormones* (Litwack, G., and Begley, T., Eds.) Vol. 61, pp 51−101, Academic Press, New York.
2. Marquet, A. (2001) Enzymology of carbon-sulfur bond formation, *Curr. Opin. Chem. Biol. 5*, 541−549.
3. Jarrett, J. T. (2005) The novel structure and chemistry of iron-sulfur clusters in the adenosylmethionine-dependent radical enzyme biotin synthase, *Arch. Biochem. Biophys. 433*, 312−321.
4. Sofia, H. J., Chen, G., Hetzler, B. G., Reyes-Spindola, J. F., and Miller, N. E. (2001) Radical SAM, a novel protein superfamily linking unresolved steps in familiar biosynthetic pathways with radical mechanisms: Functional characterization using new analysis and information visualization methods, *Nucleic Acids Res. 29*, 1097−1106.
5. Layer, G., Moser, J., Heinz, D. W., Jahn, D., and Schubert, W.-D. (2003) Crystal structure of coproporphyrinogen III oxidase reveals cofactor geometry of radical SAM enzymes, *EMBO J. 23*, 6214−6224.
6. Berkovitch, F., Nicolet, Y., Wan, J. T., Jarrett, J. T., and Drennan, C. L. (2004) Crystal structure of biotin synthase, an *S*-adenosylmethionine-dependent radical enzyme, *Science 303*, 76−79.
7. Hänzelmann, P., and Schindelin, H. (2004) Crystal structure of the *S*-adenosylmethionine-dependent enzyme MoaA and its implications for molybdenum cofactor deficiency in humans, *Proc. Natl. Acad. Sci. U.S.A. 101*, 12870−12875.
8. Lepore, B. W., Ruzicka, F. J., Frey, P. A., and Ringe, D. (2005) The X-ray crystal structure of lysine-2,3-aminomutase from *Clostridium subterminale*, *Proc. Natl. Acad. Sci. U.S.A. 102*, 13819−13824.
9. Ifuku, O., Koga, N., Haze, S., Kishimoto, J., and Wachi, Y. (1994) Flavodoxin is required for conversion of dethiobiotin to biotin in *Escherichia coli*, *Eur. J. Biochem. 224*, 173−178.
10. Birch, O. M., Fuhrmann, M., and Shaw, N. M. (1995) Biotin synthase from *Escherichia coli*, an investigation of the low molecular weight and protein components required for activity *in vitro*, *J. Biol. Chem. 270*, 19158−19165.
11. Guianvarc'h, D., Florentin, D., Tse Sum Bui, B., Nunzi, F., and Marquet, A. (1997) Biotin synthase, a new member of the family of enzymes which uses *S*-adenosylmethionine as a source of deoxyadenosyl radical, *Biochem. Biophys. Res. Commun. 236*, 402−406.
12. Shaw, N. M., Birch, O. M., Tinschert, A., Venetz, V., Dietrich, R., and Savoy, L.-A. (1998) Biotin synthase from *Escherichia coli*: Isolation of an enzyme-generated intermediate and stoichiometry of *S*-adenosylmethionine use, *Biochem. J. 330*, 1079−1085.
13. Ollagnier-de-Choudens, S., Sanakis, Y., Hewitson, K. S., Roach, P., Münck, E., and Fontecave, M. (2002) Reductive cleavage of *S*-adenosylmethionine by biotin synthase from *Escherichia coli*, *J. Biol. Chem. 277*, 13449−13454.
14. Ugulava, N. B., Sacanell, C. J., and Jarrett, J. T. (2001) Spectroscopic changes during a single turnover of biotin synthase: Destruction of a [2Fe-2S] cluster accompanies sulfur insertion, *Biochemistry 40*, 8352−8358.
15. Tse Sum Bui, B., Benda, R., Schünemann, V., Florentin, D., Trautwein, A. X., and Marquet, A. (2003) Fate of the $(2Fe\text{-}2S)^{2+}$ cluster of *Escherichia coli* biotin synthase during reaction: A Mössbauer characterization, *Biochemistry 42*, 8791−8798.
16. Sanyal, I., Cohen, G., and Flint, D. H. (1994) Biotin synthase: purification, characterization as a [2Fe-2S] cluster protein, and *in vitro* activity of the *Escherichia coli bioB* gene product, *Biochemistry 33*, 3625−3631.
17. Tse Sum Bui, B., Florentin, D., Fournier, F., Ploux, O., Méjean, A., and Marquet, A. (1998) Biotin synthase mechanism: On the origin of sulphur, *FEBS Lett. 440*, 226−230.
18. Cosper, M. M., Jameson, G. N. L., Hernandez, H. L., Krebs, C., Huynh, B. H., and Johnson, M. K. (2004) Characterization of the cofactor composition of *Escherichia coli* biotin synthase, *Biochemistry 43*, 2007−2021.
19. Ugulava, N. B., Surerus, K. K., and Jarrett, J. T. (2002) Evidence from Mössbauer spectroscopy for distinct $[2Fe\text{-}2S]^{2+}$ and $[4Fe\text{-}4S]^{2+}$ cluster binding sites in biotin synthase from *Escherichia coli*, *J. Am. Chem. Soc. 124*, 9050−9051.
20. Escalettes, F. (2000) Etude du mécanisme de la biotine synthase, Ph.D. Thesis, University Paris VI, Paris, France.
21. Jameson, G. N. L., Cosper, M. M., Hernandez, H. L., Johnson, M. K., and Huynh, B. H. (2004) Role of the [2Fe-2S] cluster in recombinant *Escherichia coli* biotin synthase, *Biochemistry 43*, 2022−2031.
22. Escalettes, F., Florentin, D., Tse Sum Bui, B., Lesage, D., and Marquet, A. (1999) Biotin synthase mechanism: Evidence for hydrogen transfer from the substrate into deoxyadenosine, *J. Am. Chem. Soc. 121*, 3571−3578.
23. Hewitson, K. S., Baldwin, J. E., Shaw, N. M., and Roach, P. L. (2000) Mutagenesis of the proposed iron-sulfur cluster binding ligands in *Escherichia coli* biotin synthase, *FEBS Lett. 466*, 372−376.
24. Hewitson, K. S., Ollagnier-de Choudens, S., Sanakis, Y., Shaw, N. M., Baldwin, J. E., Münck, E., Roach, P. L., and Fontecave, M. (2002) The iron-sulfur center of biotin synthase: Site-directed mutants, *J. Biol. Inorg. Chem. 7*, 83−93.
25. McIver, L., Baxter, R. L., and Campopiano, D. J. (2000) Identification of the [Fe-S] cluster-binding residues of *Escherichia coli* biotin synthase, *J. Biol. Chem. 275*, 13888−13894.
26. DeLano, W. L. (2002) *The PyMOL Molecular Graphics System*, DeLano Scientific, San Carlos, CA.
27. Ugulava, N. B., Gibney, B. R., and Jarrett, J. T. (2000) Iron-sulfur cluster interconversions in biotin synthase: Dissociation and reassociation of iron during conversion of [2Fe-2S] to [4Fe-4S] clusters, *Biochemistry 39*, 5206−5214.
28. Tse Sum Bui, B., Lotierzo, M., Escalettes, F., Florentin, D., and Marquet, A. (2004) Further investigation on the turnover of *Escherichia coli* biotin synthase with dethiobiotin and 9-mercaptodethiobiotin as substrates, *Biochemistry 43*, 16432−16441.
29. Izumi, Y., Osakai, M., and Yamada, H. (1987) Biotin assay using lyophilized and glycerol-suspended cultures, *J. Microbiol. Methods 6*, 237−246.
30. Tse Sum Bui, B., Mattioli, T. A., Florentin, D., Bolbach, G., and Marquet, A. (2006) *Escherichia coli* biotin synthase produces selenobiotin. Further evidence of the involvement of the $[2Fe\text{-}2S]^{2+}$ cluster in the sulfur insertion step, *Biochemistry 45*, 3824−3834.
31. Bradford, M. M. (1976) A rapid and sensitive method for the quantification of microgram quantities of protein using the principle of protein-dye binding, *Anal. Biochem. 72*, 248−254.
32. Fish, W. W. (1998) Rapid colorimetric micromethod for the quantitation of complexed iron in biological samples, *Methods Enzymol. 158*, 357−364.
33. Stephens, P. J., Thomson, A. J., Dunn, J. B., Keiderling, T. A., Rawlings, J., Rao, K. K., and Hall, D. O. (1978) Circular dichroism

and magnetic circular dichroism of iron-sulfur proteins, *Biochemistry 17*, 4770−4778.
34. Tse Sum Bui, B., Florentin, D., Marquet, A., Benda, R., and Trautwein, A. X. (1999) Mössbauer studies of *Escherichia coli* biotin synthase: Evidence for reversible interconversion between $[2Fe\text{-}2S]^{2+}$ and $[4Fe\text{-}4S]^{2+}$ clusters, *FEBS Lett. 456*, 411−414.
35. Nicolet, Y., and Drennan, C. L. (2004) AdoMet radical proteins—from structure to evolution—alignment of divergent protein sequences reveals strong secondary structure element conservation, *Nucleic Acids Res. 32*, 4015−4025.

BI060662M